P-N Approximation for Radiative Heat Transfer in a Nongray Medium

Adnan Yücel* and Yildiz Bayazitoglu†
Rice University, Houston, Texas

Using the rectangular model to characterize the spectral dependence of the absorption coefficient, the *P-N* approximation is extended to treat nongray radiative transfer problems in planar media. Specifically, the *P*-1 and *P*-3 approximation formulations are developed for a medium with any number of bands. Analytical solutions are derived for the special case of a single-level absorption coefficient. Numerical solutions are obtained for a medium with a two-level absorption coefficient. Comparisons with the available exact solutions for radiative equilibrium show that the *P*-1 and *P*-3 approximations generate accurate results. Solutions for internal heat generation are also discussed.

Nomenclature

D = the operator d/dτ
e_b = blackbody emissive power
i = intensity of radiation
i_b = blackbody intensity of radiation, e_b/π
i_k = kth moment of intensity of radiation, $k=0,1,\ldots,N$
ℓ_z = direction cosine of z direction, cosβ
L = distance between plates
q_R, Q_R = radiative heat flux, $Q_R = q_R/\sigma T_1^4$
r = position vector
s, S = rate of heat generation, $S = (s/\kappa)/\sigma T_1^4$
T = temperature
T_1 = wall temperature at $z=0$
T_2 = wall temperature at $z=$ L
z = spatial coordinate
β = polar angle
$\Delta\nu$ = bandwidth
ϵ = emissivity
θ = dimensionless temperature, T/T_1
θ_1 = dimensionless wall temperature at $z=0$
θ_2 = dimensionless wall temperature at $z=L$
κ = absorption coefficient
ν = spectral variable (frequency)
$\bar{\nu}$ = dimensionless spectral variable, $h\nu/kT_1$
$\bar{\nu}_{co}$ = dimensionless cutoff frequency for models A, B, E, and F
σ = Stefan-Boltzmann constant
τ = optical depth in z direction, κz
τ_0 = optical thickness, κL or $\max(\kappa_1,\kappa_2,\ldots,\kappa_n)z$
ϕ = azimuthal angle
ϕ = dimensionless quantity for subproblem I, Eqs. (18) and (26)
ψ = dimensionless quantity for subproblem II, Eqs. (19) and (27)
Ω = solid angle

Subscripts

j = jth band
k = kth moment of intensity
ν = spectral quantity

Received May 11, 1982; revision received Oct. 4, 1982.

*Graduate Student, Mechanical Engineering and Materials Science Department (presently Visiting Assistant Professor, Department of Mechanical Engineering, University of Mississippi, University, Miss.).

†Associate Professor, Mechanical Engineering and Materials Science Department. Member AIAA.

Introduction

An exact solution of the equation of radiative transfer may require integrations with respect to time, position, frequency, and direction. While such a solution may be accurate, its complexity makes it inconvenient for most practical problems. Many investigators have employed assumptions and approximations which led to simple solutions that are restricted in applicability. The most common assumption in the literature is that of a gray medium which eliminates the frequency dependence. Since absorption in most gases and semitransparent solids is restricted to specific intervals of the spectrum, the gray gas concept is of limited utility. Earlier attempts to take into account the nongray behavior led to the definition of various mean absorption coefficients which are restricted to certain optical conditions.[1] The study of radiative transfer in planetary atmospheres and combustion systems have resulted in detailed knowledge of the constituents such as CO, N_2O, H_2O, CH_4, NH_3, and O_3 which emit and absorb significantly in the infrared range. Various line and band models and band absorptance correlations have been developed to be used in theoretical calculations of the transmittance (or absorptance) of these gases.[1-13] Nongray radiative transfer in semitransparent solids have also received considerable attention.[14]

Even with the gray medium assumption, the mathematical difficulties encountered in working with integrodifferential equations have resulted in a number of approximate solutions to the equation of radiative transfer. One of the more elaborate schemes is the spherical harmonics method or the *P-N* approximation, first suggested by Jeans.[15] The spherical harmonics method was initially employed by astrophysicists in the problem of radiative transfer in stellar atmospheres. It was first applied to thermal radiative studies by Cheng,[16,17] who took the first order intensity approximation.

The *P*-1 approximation has been shown to give satisfactory results for a one-dimensional optically thick medium. But, it will, like the diffusion approximation, tend to overpredict the heat flux in a medium which is optically thin. Higher-order approximations would retain the differential nature of the approximation and result in more accurate solutions than those obtained from the first-order approximation. Increasing the number of terms, however, also complicates the solution process. Higher-order approximations were used in solving various one- and two-dimensional radiative transfer problems in planar, spherical, and cylindrical media.[18-22] The *P*-3 approximation yields satisfactory solutions over the whole range of optical thickness in planar geometries.[19,21] Bayazitoglu and Higenyi[19] have shown that the *P-N* approximation is less accurate in nonplanar media.

Despite its effectiveness in generating accurate approximate solutions to the gray radiative transfer problem, little work

has been done to generalize the *P-N* approximation for nongray problems. The challenge here lies in the integration of the moment equations over the spectral variable. The differential form of these equations precludes the use of band absorptance correlations which are tailored for the integral formulation. Modest[23] has combined a box model with the *P*-1 approximation. The results show good comparison for the case of radiative equilibrium. Kung and Sibulkin[24] have used the differential approximation to obtain approximate solutions in a radiating medium with a two-level absorption coefficient. In another approach, Yuen and Rasky[25] have applied the *P*-1 approximation to a nongray medium by formulating the problem in terms of the spectral coefficient. Their results obtained by approximating the spectral moments of intensity by specific polynomials compare well with the exact results for the case of radiative equilibrium.

The purpose of this study is to develop and solve the differential relations for nongray radiative transfer in a participating planar medium. The *P*-1 and *P*-3 approximations will be used to represent the angular distribution of the radiation intensity. The rectangular model will be employed to characterize the spectral variations of the absorption coefficient. The rectangular model can be readily introduced into the *P-N* approximation formulation. Although less realistic than other band models, its accuracy can be improved by dividing the spectrum into smaller intervals. Multiband cases are easily handled. It is also applicable to those media for which band absorptance correlations are not available or the use of narrow-band approximation is not justifiable. Marshak boundary conditions are used to complete the formulation. Solutions will be obtained for various radiative transfer problems. Results will be compared to the available exact solutions and the accuracy of the approximations will be assessed.

Formulation

The physical system under consideration consists of an absorbing, emitting, and nonscattering medium bounded by two infinite parallel plates. The medium is in local thermodynamic equilibrium and has a refractive index of unity. The absorption coefficient of the medium is spectrally dependent. The medium is capable of generating heat at a rate of s per unit of volume. Steady state is assumed. The plate at $z=0$ (lower boundary) is maintained at temperature T_1 and the other at $z=L$ (upper boundary) at temperature T_2. Throughout this work T_1 is greater than T_2. The opaque boundaries are assumed to be diffusely emitting and reflecting surfaces.

The equation of radiative transfer governing this one dimensional planar system is

$$\ell_z \mathrm{d}i_\nu/\mathrm{d}z = -\kappa_\nu i_\nu + \kappa_\nu i_{b\nu} \tag{1}$$

In the spherical harmonics method, the intensity of radiation is expanded in an orthogonal series of the spherical harmonics[19]

$$i_\nu(r;\beta,\phi) = \sum_{n=0}^{\infty}\sum_{m=0}^{n} \frac{2n+1}{4\pi} P_n^m(\cos\beta)\,[A_n^m(r,\nu)\cos m\phi + D_n^m(r,\nu)\sin m\phi] \tag{2}$$

where $P_n^m(\cos\beta)$ are the associated Legendre polynomials of the first kind. In practice, the series is truncated after a certain (N) number of terms (hence the *P-N* approximation) such that $A_n^m = D_n^m = 0$ for $n>N$. The coefficients A_n^m and D_n^m up to $N=3$ are given in Table 1. For one-dimensional geometry under azimuthal symmetry the intensity distributions for the *P*-3 approximation are

$$4\pi i_\nu(z) = i_{0\nu}(z) + 3i_{1\nu}(z)P_1^0(\cos\beta) + \frac{5}{2}[3i_{2\nu}(z) - i_{0\nu}(z)]P_2^0(\cos\beta) + \frac{7}{2}[5i_{3\nu}(z) - 3i_{1\nu}(z)]P_3^0(\cos\beta) \tag{3}$$

The intensity distribution for the *P*-1 approximation corresponds to the first two terms of the above equation, in which the relevant coefficients A_n^m and D_n^m have been replaced by their equivalents in terms of the moments of intensity. The kth moment of intensity in the z direction is defined as

$$i_{k\nu}(z) = \int_\Omega i_\nu \ell_z^k \mathrm{d}\Omega, \qquad k=0,1,\ldots,N \tag{4a}$$

Of particular interest is the first moment of intensity which physically signifies the spectral radiative flux in the z direction.

$$q_{R\nu} \equiv i_{1\nu} = \int_\Omega i_\nu \ell_z \mathrm{d}\Omega \tag{4b}$$

The differential equations governing the moments of intensity in the *P-N* approximation are obtained by multiplying the equation of transfer by the appropriate powers of the direction cosine and integrating over all solid angles. Equations of the *P*-3 approximation are

$$\frac{\mathrm{d}i_{1\nu}}{\mathrm{d}z} = \kappa_\nu(4e_{b\nu} - i_{0\nu}) \tag{5a}$$

$$\frac{\mathrm{d}i_{2\nu}}{\mathrm{d}z} = -\kappa_\nu i_{1\nu} \tag{5b}$$

$$\frac{\mathrm{d}i_{3\nu}}{\mathrm{d}z} = \kappa_\nu(4e_{b\nu}/3 - i_{2\nu}) \tag{5c}$$

$$\frac{\mathrm{d}i_{4\nu}}{\mathrm{d}z} = -\kappa_\nu i_{3\nu} \tag{5d}$$

and the closure condition is

$$i_{4\nu} = 6i_{2\nu}/7 - 3i_{0\nu}/35 \tag{6}$$

The boundary conditions obtained by using the Marshak[26] approach are

$$3\epsilon_\nu i_{0\nu} \pm 16(2-\epsilon_\nu)i_{1\nu} + 15\epsilon_\nu i_{2\nu} = 32\epsilon_\nu e_{b\nu} \tag{7a}$$

$$(3\epsilon_\nu - 5)i_{0\nu} \pm 16(1-\epsilon_\nu)i_{1\nu} + 15(1+\epsilon_\nu)i_{2\nu} \pm 32i_{3\nu} = 32\epsilon_\nu e_{b\nu} \tag{7b}$$

where the plus sign corresponds to the lower boundary and the minus sign to the upper boundary.

Equations (5a) and (5b) consitute the governing equations and Eq. (7a) the boundary conditions for the *P*-1 approximation, with the closure condition given by

$$i_{2\nu} = i_{0\nu}/3 \tag{8}$$

In order to integrate Eqs. (5) over the spectral variable, the spectral dependence of the absorption coefficient of the medium must be known. In many gases and semitransparent solids, absorption is restricted to specific intervals of the

Table 1 Coefficients A_n^m and D_n^m in terms of the moments of intensity[a,b]

	m	$n=0$	$n=1$	$n=2$	$n=3$
A_n^m	0	i_0	i_z	$(3i_{zz}-i_0)/2$	$(5i_{zzz}-3i_z)/2$
	1	—	i_x	i_{xz}	$(5i_{xzz}-i_x)/4$
	2	—	—	$(i_{xx}-i_{yy})/4$	$(i_{zxx}-i_{zyy})/4$
	3	—	—	—	$(i_{xxx}-i_{xyy})/24$
D_n^m	1	—	i_y	i_{zy}	$(5i_{yzz}-i_y)/4$
	2	—	—	$i_{xy}/2$	$i_{xyz}/2$
	3	—	—	—	$(3i_{yxx}-i_{yyy})/24$

[a] Coefficients A_n^m and D_n^m can be adapted to cylindrical or spherical coordinates by replacing the subscripts in Cartesian coordinates $\{z,x,y\}$ with $\{z,r,\theta\}$ in cylindrical coordinates and $\{r,\theta,\phi\}$ in spherical coordinates. The following relations will also hold. $i_0=i_{xx}+i_{yy}+i_{zz}$, $i_s=i_{sxx}+i_{syy}+i_{szz}$, $s=x$, y, or z.
[b] In this study: $i_1=i_z$, $i_2=i_{zz}$, $i_3=i_{zzz}$.

spectrum. Among the many models, the rectangular model is the simplest one that can be used in such physical situations. In this model, the spectral absorption coefficient is assumed to be constant over certain intervals.

Given the rectangular model for the spectral variation of the absorption coefficient, the moment equations and the boundary conditions for the P-1 and P-3 approximations can be integrated over the spectral variable for each band. Introducing the closure conditions given by Eqs. (6) and (8), the integrated form of the moment equations are

P-1 Approximation

$$\frac{di_{0j}}{dz}=-3\kappa_j i_{1j} \tag{9a}$$

$$\frac{di_{1j}}{dz}=\kappa_j(4e_{bj}-i_{0j}) \tag{9b}$$

P-3 Approximation

$$\frac{di_{0j}}{dz}=\kappa_j(-10i_{1j}+35i_{3j}/3) \tag{10a}$$

$$\frac{di_{1j}}{dz}=\kappa_j(4e_{bj}-i_{0j}) \tag{10b}$$

$$\frac{di_{2j}}{dz}=-\kappa_j i_{1j} \tag{10c}$$

$$\frac{di_{3j}}{dz}=\kappa_j(4e_{bj}/3-i_{2j}) \tag{10d}$$

where

$$i_{kj}=\int_{\Delta\nu_j} i_{k\nu}d\nu, \qquad k=0,1,\ldots,N \tag{11a}$$

$$e_{bj}=\int_{\Delta\nu_j} e_{b\nu}d\nu, \qquad j=1,2,..,n \tag{11b}$$

The respective integrated boundary conditions for the P-1 and P-3 approximations are

$$\epsilon i_{0j}\pm 2(2-\epsilon)i_{1j}=4\epsilon e_{bj} \tag{12}$$

and

$$3\epsilon i_{0j}\pm 16(2-\epsilon)i_{1j}+15\epsilon i_{2j}=32\epsilon e_{bj} \tag{13a}$$

$$(3\epsilon-5)i_{0j}\pm 16(1-\epsilon)i_{1j}+15(1+\epsilon)i_{2j}\pm 32i_{3j}=32\epsilon e_{bj} \tag{13b}$$

where the boundaries are assumed to be gray. In order to reduce the number of independent parameters in these problems, the boundaries will be assumed to be black (i.e., $\epsilon_1=\epsilon_2=1$), although the expressions for the boundary conditions may retain their general form. The total radiative flux given by

$$q_R=\int_0^\infty i_{1\nu}d\nu \tag{14a}$$

can now be expressed as

$$q_R=\sigma T_1^4-\sigma T_2^4+\sum_{j=1}^n i_{1j}-\sum_{j=1}^n [e_{bj}(T_1)-e_{bj}(T_2)] \tag{14b}$$

For a purely radiating medium with uniform heat generation, the conservation of energy equation is

$$\frac{dq_R}{dz}=s \tag{15a}$$

Combining Eqs. (9b) or (10b) with Eq. (14a) we have

$$\frac{dq_R}{dz}=\sum_{j=1}^n\frac{di_{1j}}{dz}=\sum_{j=1}^n\kappa_j(4e_{bj}-i_{0j})=s \tag{15b}$$

Analysis and Discussion of Results for Various Rectangular Models

In this section various rectangular model configurations will be considered and the heat transfer results will be presented to show the effects of nongrayness. Wherever possible, the P-1 and P-3 solutions will be compared with the exact solutions and the accuracy of these approximations will be discussed.

n Bands with Identical Absorption Coefficients

A special case merits attention when conduction is negligible. If the absorption coefficients for each band are identical, i.e., $\kappa_j=\kappa=$const, the moment equations and the boundary conditions for each band can be summed to yield a single set of differential equations and boundary conditions for the total quantities

$$i_{kt}=\sum_{j=1}^n i_{kj}, \qquad k=0,1,\ldots,N \tag{16a}$$

and

$$e_{bt}=\sum_{j=1}^n e_{bj} \tag{16b}$$

In general this system of equations is nonlinear. If the absorption coefficient is independent of the temperature, the system becomes linear and superposition can be used to divide the general problem into two subproblems[10]:

Subproblem I: lower boundary at T_1, upper boundary at T_2, no heat generation.

Subproblem II: lower boundary at T_2, upper boundary at T_2, uniform heat generation.

P-1 Formulation

We define

$$e_{bt}=(e_1-e_2)\phi_b+(s/\kappa)\psi_b+e_2 \tag{17a}$$

$$i_{0t}=(e_1-e_2)\phi_0+(s/\kappa)\psi_0+4e_2 \tag{17b}$$

$$i_{1t}=(e_1-e_2)\phi_1+(s/\kappa)\psi_1 \tag{17c}$$

The dimensionless quantities ϕ and ψ that correspond to subproblems I and II, respectively, are defined as

$$\phi_b = [(e_{bt})_{\rm I} - e_2]/(e_1 - e_2) \tag{18a}$$

$$\phi_0 = [(i_{0t})_{\rm I} - 4e_2]/(e_1 - e_2) \tag{18b}$$

$$\phi_1 = (i_{1t})_{\rm I}/(e_1 - e_2) \tag{18c}$$

$$\psi_b = [(e_{bt})_{\rm II} - e_2]/(s/\kappa) \tag{19a}$$

$$\psi_0 = [(i_{0t})_{\rm II} - 4e_2]/(s/\kappa) \tag{19b}$$

$$\psi_1 = (i_{1t})_{\rm II}/(s/\kappa) \tag{19c}$$

where $e_1 = e_{bt}(T_1)$, $e_2 = e_{bt}(T_2)$.

Substituting Eqs. (17) in the moment equations and the boundary conditions, we obtain

$$DI_0 = -3I_1 \tag{20a}$$

$$DI_1 = F \tag{20b}$$

$$I_0 + 2(2/\epsilon_1 - 1)I_1 = 4B \qquad \text{at } \tau = 0 \tag{21a}$$

$$I_0 - 2(2/\epsilon_2 - 1)I_1 = 0 \qquad \text{at } \tau = \tau_0 \tag{21b}$$

where $\tau = \kappa z$, $D \equiv (\mathrm{d}/\mathrm{d}\tau)$, and $\tau_0 = \kappa L$.

From Eq. (15b), we obtain

$$4I_b - I_0 = F \tag{22}$$

In the above expressions, I corresponds to ϕ and ψ, and B takes the values 1 and 0, respectively, in subproblems I and II, where $F = 1 - B$.

Equations (20) can be integrated to yield

$$I_0(\tau) = -3F\tau^2/2 - 3c_1 + c_2 \tag{23a}$$

$$I_1(\tau) = F\tau + c_1 \tag{23b}$$

The integration constants c_1 and c_2 are evaluated through the boundary conditions [Eq. (21)].

$$c_1 = (4B - 3F\tau_0^2/2 - 2E_2F\tau_0)/(3\tau_0 + 2E_1 + 2E_2) \tag{24a}$$

$$c_2 = 4B - 2E_1c_1 \tag{24b}$$

where $E_1 = 2/\epsilon_1 - 1$, $E_2 = 2/\epsilon_2 - 1$.

P-3 Formulation

In addition to definitions of e_{bt}, i_{0t}, and i_{1t} given by Eqs. (17), we define

$$i_{2t} = (e_1 - e_2)\phi_2 + (s/\kappa)\psi_2 + 4e_2/3 \tag{25a}$$

$$i_{3t} = (e_1 - e_2)\phi_3 + (s/\kappa)\psi_3 \tag{25b}$$

where

$$\phi_2 = [(i_{2t})_{\rm I} - 4e_2/3]/(e_1 - e_2) \tag{26a}$$

$$\phi_3 = (i_{3t})_{\rm I}/(e_1 - e_2) \tag{26b}$$

$$\psi_2 = [(i_{2t})_{\rm II} - 4e_2/3]/(s/\kappa) \tag{27a}$$

$$\psi_3 = (i_{3t})_{\rm II}/(s/\kappa) \tag{27b}$$

Substituting Eqs. (17) and (25) in the moment differential equations and the boundary conditions for the $P-3$ approximation, we obtain

$$DI_0 = -10I_1 + (35/3)I_3 \tag{28a}$$

$$DI_1 = F \tag{28b}$$

$$DI_2 = -I_1 \tag{28c}$$

$$DI_3 = 4I_b/3 - I_2 \tag{28d}$$

and

$$3\epsilon_1 I_0 + 16(2 - \epsilon_1)I_1 + 15\epsilon_1 I_2 = 32\epsilon_1 B \tag{29a}$$

$$(3\epsilon_1 - 5)I_0 + 16(1 - \epsilon_1)I_1 + 15(1 + \epsilon_1)I_2 + 32I_3 = 32\epsilon_1 B \text{ at } \tau = 0 \tag{29b}$$

$$3\epsilon_2 I_0 - 16(2 - \epsilon_2)I_1 + 15\epsilon_2 I_2 = 0 \tag{29c}$$

$$(3\epsilon_2 - 5)I_0 - 16(1 - \epsilon_2)I_1 + 15(1 + \epsilon_2)I_2 - 32I_3 = 0 \text{ at } \tau = \tau_0 \tag{29d}$$

The conservation of energy equation is identical to Eq. (22).

Equations (28) can be combined to yield a single fourth-order differential equation for I_0

$$D^4 I_0 - 35D^2 I_0/9 = 35F/3 \tag{30}$$

The general solution of this equation is

$$I_0(\tau) = -3F\tau^2/2 + D_1 + D_2\tau + D_3\cosh(\sqrt{35}\tau/3) + D_4\sinh(\sqrt{35}\tau/3) \tag{31}$$

where D_1 through D_4 are integration constants to be determined via the boundary conditions given in Eqs. (29).

From Eqs. (20) and (28) we observe that the function vectors ϕ and ψ are identical to those derived for a gray medium.[19,21] Therefore functions ϕ and ψ are general solutions of a class of problems for which the gray problem is a limiting case. The same also holds for the exact formulation of the problem in which the energy equation is reduced to the same linear Fredholm-type integral equation of the second kind governing the temperature field in a gray medium.[10]

Hence when the absorption coefficient has only one nonzero value, the dimensionless heat flux (ϕ_1, ψ_1) and emissive power (ϕ_b, ψ_b) distributions given by the P-N approximation will be the same whether the medium is gray or "fractionally" gray. The influence of the nongrayness occurs in the terms e_1 and e_2 appearing in Eqs. (17) and (25).

Since the emissive power and radiative flux distributions for the gray case have been thoroughly discussed in the literature,[19,21] they will be only briefly mentioned here. As would be expected, P-3 approximation is superior to the P-1 approximation over the whole range of the optical thickness in predicting the emissive power and the radiative flux. P-1 approximation approaches the exact solution as the medium becomes optically thick. The largest errors occur at the boundaries where both approximations tend to underestimate the emissive power near the hot boundary and overestimate it in the vicinity of the cold boundary. The largest deviations in the radiative flux results are for the optically thin medium. However, the P-N approximations yield the correct results as the optical thickness approaches zero.

To show the effect of nongrayness, two simple models for the absorption coefficient will be considered. These are

Model A

$$\kappa_\nu = \kappa \quad \text{for} \quad 0 \le \nu \le \nu_{co}$$

$$\kappa_\nu = 0 \quad \text{for} \quad \nu_{co} > 3$$

Model B

$$\kappa_\nu = 0 \quad \text{for} \quad 0 \le \nu < \nu_{co}$$

$$\kappa_\nu = \kappa \quad \text{for} \quad \nu \ge \nu_{co}$$

Note that when ν_{co}, the cutoff frequency, goes to infinity in model A or approaches zero in model B, the medium becomes gray. In Table 2, the radiative flux results for the case of radiative equilibrium are compared with the exact results.[10] Both approximations predict the radiative flux very well, especially at large optical depths.

Once the functions ϕ_b and ψ_b are known, the medium temperature can be determined by solving Eq. (17a). The temperature distributions for the case with $S=0$, $\theta_2=0.5$, $\tau_0=1$, and $\bar{\nu}_{co}=3$ are shown in Fig. 1, along with the exact results.[10] The curves are almost identical in the central part of the medium. It should be noted that both the exact and the P-1 and P-3 approximation solutions yield the identical result $\phi_b(\tau_0/2)=0.5$ for all τ_0. We observe that the discrepancy in the emissive powers at the walls is reflected in the temperature distributions. The relative errors evaluated at the walls do not exceed 4%. Figure 2 displays the effect of optical thickness on the temperature. The temperature distribution for model A is always located under the gray solution. Conversely, the temperature for model B lies above the gray solution. As in the gray case, the temperature jump at the boundaries disappears with increasing optical depths.

Two Bands with Different Absorption Coefficients

In order to demonstrate the effects of a more general function for κ_ν, two simple models will be employed. These models are shown in Fig. 3. A two-level model for the absorption coefficient similar to model E was employed in the study of radiating shock layers[27] and also in stellar atmosphere problems. Note that models E and F reduce to models A and B, respectively, when $\alpha=0$, while they both correspond to the gray model when $\alpha=1$.

Unlike the previous case, the problem becomes nonlinear with the multilevel absorption coefficient model. Analytical solutions cannot be obtained. Equations (9) and (10), together

Table 2 Effect of cutoff frequency ν_{co} on the dimensionless radiative flux Q_R: models A and B, $\theta_2=0.5$ (radiation equilibrium)

Model	$\bar{\nu}_{co}$		$\tau_0=0.1$	$\tau_0=1$	$\tau_0=10$
A	2	Ex[a]	0.9254	0.8733	0.8104
		P-3	0.9262	0.8736	0.8105
		P-1	0.9275	0.8759	0.8106
	3	Ex	0.9089	0.7860	0.6378
		P-3	0.9109	0.7868	0.6379
		P-1	0.9138	0.7921	0.6381
	5	Ex	0.8791	0.6282	0.3257
		P-3	0.8832	0.6298	0.3258
		P-1	0.8892	0.6407	0.3264
Gray	—	Ex	0.8585	0.5188	0.1095
		P-3	0.8641	0.5210	0.1096
		P-1	0.8721	0.5357	0.1103
B	2	Ex	0.8706	0.5831	0.2365
		P-3	0.8753	0.5849	0.2366
		P-1	0.8821	0.5974	0.2372
	3	Ex	0.8871	0.6703	0.4091
		P-3	0.8906	0.6717	0.4092
		P-1	0.8958	0.6811	0.4096
	5	Ex	0.9169	0.8281	0.7212
		P-3	0.9183	0.8287	0.7213
		P-1	0.9204	0.8326	0.7214

[a] Exact results obtained from Ref. 10.

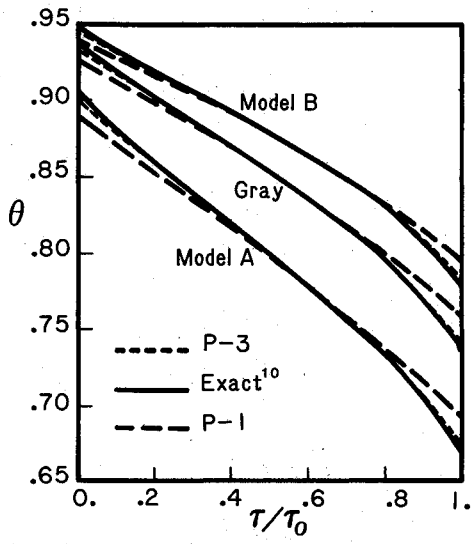

Fig. 1 Dimensionless temperature distributions for models A and B: $\bar{\nu}_{co}=3$, $\tau_0=1$, $\theta_2=0.5$ (radiative equilibrium).

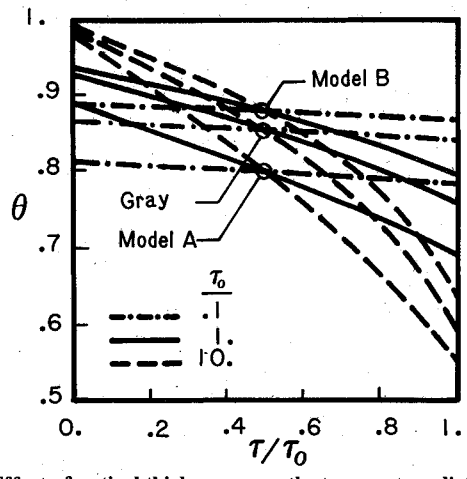

Fig. 2 Effect of optical thickness τ_0 on the temperature distributions for models A and B: $\bar{\nu}_{co}=3$, $\theta_2=0.5$ (radiative equilibrium; P-1 approximation results).

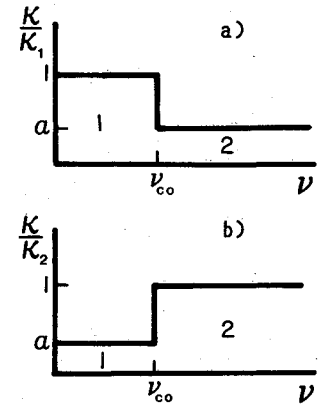

Fig. 3 Models E and F for the spectral absorption coefficient: a) model E, b) model F.

with their respective boundary conditions, constitute a nonlinear two-point boundary value problem with a non-differential constraint given by Eq. (15).

The nonlinear problem was solved by the modified quasilinearization algorithm.[28] In this algorithm, the resulting linear two-point boundary value problem is solved by the method of particular solutions. Hamming's method was used to integrate the first-order differential equation system. In determining the convergence, a performance index P was used which represents the cumulative error in the equations and the boundary conditions. The algorithm was stopped when $P \leq 10^{-16}$. Rapid convergence was achieved in all cases. Details can be found in Ref. 29.

In Tables 3 and 4, the P-1 and P-3 approximation results for the radiative equilibrium temperature and radiative heat flux are compared with the exact results[11] for various values of α. It is observed that both approximations are quite accurate for the whole range of α. Figure 4 shows the variation of the dimensionless heat flux with α. Maximum error in the P-1 approximation is about 3.4%. It is less than 1% for the P-3 approximation. The P-3 approximation matches the exact results within the accuracies associated with plotting Fig. 4.

When the medium generates heat at a constant rate, the local radiative flux is given by

$$Q_R(\tau) = S(\tau - \tau_0) + C \tag{32}$$

where C is the integration constant.

Dimensionless radiative flux evaluated at the cold wall [i.e., $Q_R(\tau_0) = C$] are plotted in Fig. 5 (model E) and Fig. 6

Table 3 Dimensionless temperatures and radiative flux Q_R: model E, $\bar{\nu}_{co} = 3$, $\tau_0 = 1$, $\theta_2 = 0.5$ (radiative equilibrium)

τ/τ_0		$\alpha=0$	$\alpha=0.05$	$\alpha=0.1$	$\alpha=0.3$	$\alpha=0.5$	$\alpha=0.9$	$\alpha=1$
0	Ex[a]	0.9072	0.9086	0.9098	0.9164	0.9235	0.9353	0.9377
	P-3	0.9019	0.9039	0.9051	0.9110	0.9184	0.9313	0.9340
	P-1	0.8895	0.8930	0.8951	0.9018	0.9090	0.9222	0.9250
0.2	Ex	0.8600	0.8682	0.8734	0.8852	0.8922	0.9014	0.9031
	P-3	0.8609	0.8690	0.8738	0.8849	0.8921	0.9020	0.9036
	P-1	0.8540	0.8624	0.8677	0.8792	0.8863	0.8695	0.8985
0.5	Ex	0.7977	0.8146	0.8247	0.8421	0.8484	0.8532	0.8537
	P-3	0.7977	0.8146	0.8250	0.8428	0.8489	0.8533	0.8537
	P-1	0.7977	0.8132	0.8232	0.8417	0.8483	0.8532	0.8537
0.8	Ex	0.7296	0.7532	0.7674	0.7900	0.7954	0.7948	0.7939
	P-3	0.7286	0.7524	0.7674	0.7915	0.7962	0.7941	0.7930
	P-1	0.7366	0.7580	0.7721	0.7971	0.8032	0.8018	0.8005
1	Ex	0.6683	0.6937	0.7095	0.7357	0.7408	0.7357	0.7334
	P-3	0.6757	0.7020	0.7190	0.7469	0.7511	0.7438	0.7411
	P-1	0.6925	0.7163	0.7324	0.7612	0.7670	0.7609	0.7581
Q_R	Ex	0.7860	0.7604	0.7376	0.6644	0.6101	0.5336	0.5188
	P-3	0.7868	0.7640	0.7426	0.6697	0.6141	0.5360	0.5210
	P-1	0.7921	0.7719	0.7526	0.6848	0.6305	0.5512	0.5357

[a] Exact results obtained from Ref. 11.

Table 4 Dimensionless temperatures and radiative flux Q_R: model F, $\bar{\nu}_{co} = 3$, $\tau_0 = 1$, $\theta_2 = 0.5$ (radiative equilibrium)

τ/τ_0		$\alpha = 0$	$\alpha=0.1$	$\alpha=0.4$	$\alpha=0.5$	$\alpha=0.6$	$\alpha=0.8$	$\alpha=1$
0	Ex[a]	0.9483	0.9426	0.9364	0.9359	0.9359	0.9365	0.9377
	P-3	0.9452	0.9389	0.9319	0.9315	0.9316	0.9325	0.9340
	P-1	0.9377	0.9315	0.9235	0.9228	0.9227	0.9234	0.9250
0.2	Ex	0.9195	0.9125	0.9043	0.9034	0.9029	0.9027	0.9031
	P-3	0.9200	0.9129	0.9043	0.9033	0.9030	0.9031	0.9036
	P-1	0.9156	0.9090	0.8996	0.8985	0.8979	0.8978	0.8985
0.5	Ex	0.8781	0.8710	0.8604	0.8585	0.8571	0.8550	0.8537
	P-3	0.8781	0.8709	0.8600	0.8581	0.8567	0.8548	0.8537
	P-1	0.8781	0.8715	0.8606	0.8586	0.8570	0.8550	0.8537
0.8	Ex	0.8272	0.8114	0.8091	0.8059	0.8030	0.7981	0.7939
	P-3	0.8264	0.8207	0.8086	0.8054	0.8024	0.7973	0.7930
	P-1	0.8329	0.8275	0.8160	0.8129	0.8101	0.8050	0.8005
1	Ex	0.7744	0.7712	0.7558	0.7554	0.7500	0.7414	0.7334
	P-3	0.7812	0.7779	0.7663	0.7621	0.7577	0.7492	0.7411
	P-1	0.7962	0.7925	0.7815	0.7776	0.7737	0.7658	0.7581
Q_R	Ex	0.6703	0.6427	0.5846	0.5702	0.5576	0.5362	0.5188
	P-3	0.6717	0.6464	0.5882	0.5734	0.5604	0.5386	0.5210
	P-1	0.6811	0.6585	0.6037	0.5891	0.5761	0.5538	0.5357

[a] Exact results obtained from Ref. 11.

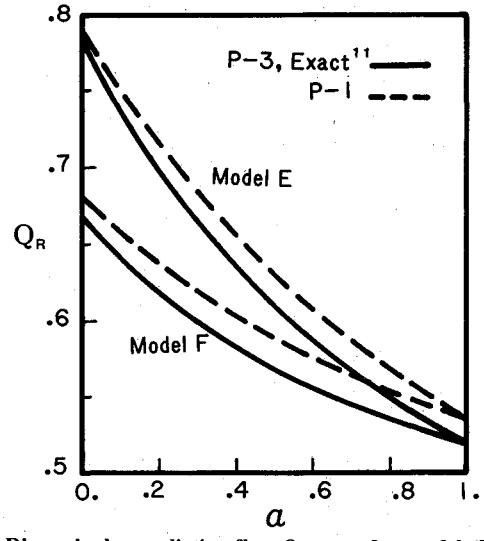

Fig. 4 Dimensionless radiative flux Q_R vs α for models E and F: $\bar{\nu}_{co}=3$, $\tau_0=1$, $\theta_2=0.5$ (radiative equilibrim).

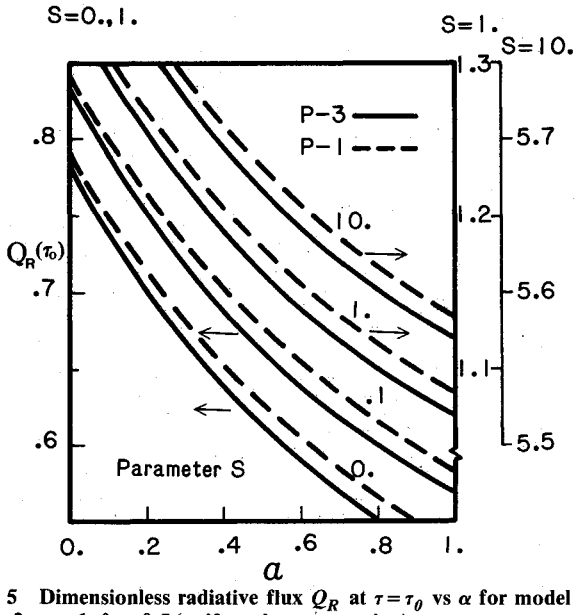

Fig. 5 Dimensionless radiative flux Q_R at $\tau=\tau_0$ vs α for model E: $\bar{\nu}_{co}=3$, $\tau_0=1$, $\theta_2=0.5$ (uniform heat generation).

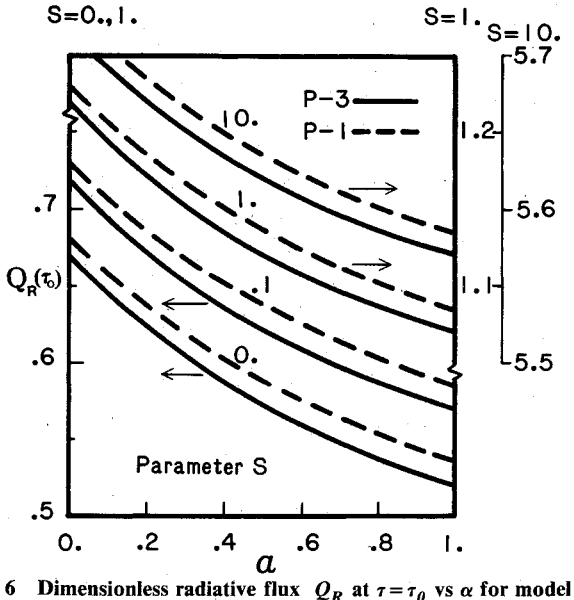

Fig. 6 Dimensionless radiative flux Q_R at $\tau=\tau_0$ vs α for model F: $\bar{\nu}_{co}=3$, $\tau_0=1$, $\theta_2=0.5$ (uniform heat generation).

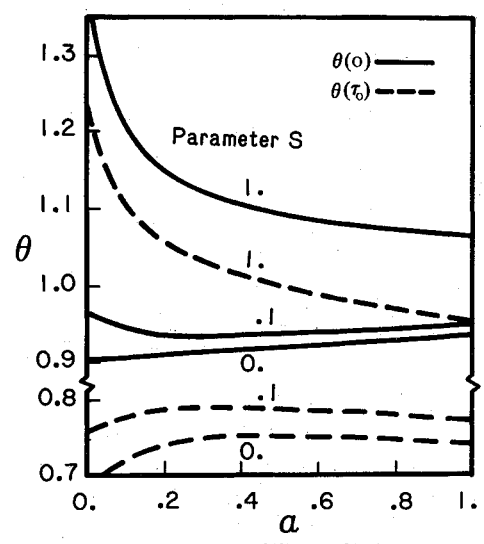

Fig. 7 Dimensionless temperatures $\theta(0)$ and $\theta(\tau_0)$ vs α for model E: $\bar{\nu}_{co}=3$, $\tau_0=1$, $\theta_2=0.5$ (uniform heat generation, P-3 approximation results).

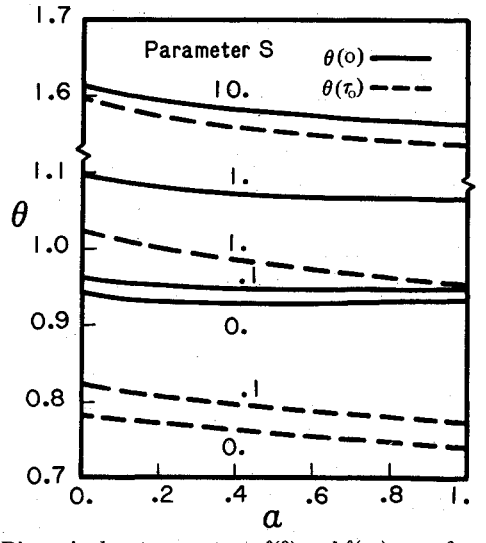

Fig. 8 Dimensionless temperatures $\theta(0)$ and $\theta(\tau_0)$ vs α for model F: $\bar{\nu}_{co}=3$, $\tau_0=1$, $\theta_2=0.5$ (uniform heat generation, P-3 approximation results).

(model F) for various values of S, the dimensionless rate of heat generation. In Fig. 5 the curves for $S=0$ represent the radiative equilibrium results given in Fig. 4. For $S\neq 0$, it is observed that the curves shift almost parallel to each other with increasing values of S. For the limiting values of $\alpha=1$ (gray case) and $\alpha=0$ (model A), the problem reduces to the linear case in which the value of the dimensionless radiative flux is directly proportional to the rate of heat generation as given by Eq. (17c). For a gray medium with uniform heat generation, Ratzel[21] has shown that the P-1 and P-3 approximations have the same order of accuracy as in the case of radiative equilibrium. This is also true for the case $\alpha=0$ (model A). Considering the established accuracy of the approximations for the limiting cases, 1) $\alpha=0$ and $\alpha=1$, $S\geq 0$, and 2) $S=0$, $0\leq\alpha\leq 1$, and judging from the behavior of the curves in Fig. 5, the P-1 and P-3 approximations can be expected to be accurate in the range $0\leq\alpha\leq 1$ for $S>0$. Similar trends in the results for model F presented in Fig. 6 lead to the same conclusion.

Significant changes occur in the variation of temperature with α when there is uniform heat generation in the medium. Variations in the medium temperatures at the walls are given in Fig. 7 (model E) and in Fig. 8 (model F). For model E,

when $S=0$, $\theta(0)$ decreases almost linearly with α from the gray case ($\alpha=1$) to the result for model A ($\alpha=0$). On the other hand, $\theta(\tau_0)$ has a value greater than the gray case[11] for $\alpha>0.26$. When $S\neq 0$, $\theta(0)$ shows a rapid increase at small values of α with increasing values of S. Observe that the curve for $S=0.1$ shows a minimum with respect to α at about $\alpha=0.2$ which disappears for $S\geq 1.0$. The maximum in $\theta(\tau_0)$ which respect to α is also displaced. Both $\theta(0)$ and $\theta(\tau_0)$ become bounded from below by the gray case with increasing heat generation in the medium. The variations in the temperature for model F show similar behavior, although they are not as strong as those for model E. From Figs. 7 and 8 we observe the temperatures for model A($\alpha=0$ in model E) surpass those for model B ($\alpha=0$ in model F) with increasing rate of heat generation, while they are both higher than those for the gray case. The reason for this is that, in a medium with a single band, only a certain spectral interval (rather than the whole spectrum in the case of a gray medium) has to account for the heat generation in the medium. This results in higher temperatures in a nongray medium with significant heat generations.

Conclusions

The P-1 and P-3 spherical harmonics approximations to the radiation intensity were used for radiative energy transfer in one-dimensional planar geometry. In a purely radiating medium with a single-valued absorption coefficient, the problem was reduced to the gray problem. A two-level absorption coefficient model was also employed. Contrary to the exact formulations, the differential character of the approximations enabled the use of conventional methods and developed algorithms in obtaining numerical solutions. Results were compared with the available exact solutions. The P-3 approximation is superior to the P-1 approximation in yielding more accurate and consistent results over the whole range of the optical thickness. The P-1 approximation may be practical in making rapid qualitative assessments or in obtaining initial estimates of the temperature for exact numerical solutions.

Acknowledgment

This work was performed under the auspices of National Science Foundation Grant ENG-7827611.

References

[1] Tien, C. L., "Thermal Radiation Properties of Gases," *Advances in Heat Transfer,* Vol. 5, 1968, pp. 253-324.

[2] Cess, R. D. and Tiwari, S. N., "Infrared Radiative Transfer in Gases," *Advances in Heat Transfer,* Vol. 8, 1972, pp. 229-283.

[3] Edwards, D. K., "Molecular Gas Band Radiation," *Advances in Heat Transfer,* Vol. 12, 1976, pp. 116-195.

[4] Tiwari, S. N., "Models for Infrared Atmospheric Radiation," *Advances in Heat Transfer,* Vol. 20, 1978, pp. 1-85.

[5] Penner, S. S., *Quantitative Molecular Spectroscopy and Gas Emissivities,* Addison-Wesley Publishing Co., Reading, Mass., 1959.

[6] Crosbie, A. L. and Viskanta, R., "Nongray Radiative Transfer in a Planar Medium Exposed to a Collimated Flux," *Journal of Quantitative Spectroscopy and Radiative Transfer,* Vol. 10, May 1970, pp. 465-485.

[7] Crosbie, A. L. and Viskanta, R., "Effect of Band or Line Shape on the Radiative Transfer in a Nongray Planar Medium," *Journal of Quantitative Spectroscopy and Radiative Transfer,* Vol. 10, May 1970, pp. 487-509.

[8] Cess, R. D., Mighdoll, P., and Tiwari, S. N., "Infrared Radiative Transfer in Nongray Gases," *International Journal of Heat Mass Transfer,* Vol. 10, Nov. 1967, pp. 1521-1532.

[9] Chan, S. H. and Tien, C. L., "Infrared Radiative Heat Transfer in Nongray Nonisothermal Gases," *International Journal of Heat Mass Transfer,* Vol. 14, Jan. 1971, pp. 19-26.

[10] Crosbie, A. L. and Viskanta, R., "The Exact Solution to a Simple Nongray Radiative Transfer Problem," *Journal of Quantitative Spectroscopy and Radiative Transfer,* Vol. 9, May 1969, pp. 553-568; also personal communication with A. L. Crosbie, Feb. 1982.

[11] Crosbie, A. L. and Viskanta, R., "Rectangular Model for Nongray Radiative Transfer," *AIAA Journal,* Vol. 8, Nov. 1970, pp. 2055-2057.

[12] Crosbie, A. L. and Viskanta, R., "Interaction of Heat Transfer by Conduction and Radiation in a Nongray Planar Medium," *Wärme- und Stoffübertragung,* Vol. 4, 1971, pp. 205-212.

[13] Siewert, C. E. and Zweifel, P. F., "An Exact Solution of Equations for Local Thermodynamic Equilibrium in the Non-Gray Case: Picket Fence Approximation," *Annals of Physics,* Vol. 36, Jan. 1966, pp. 61-87.

[14] Viskanta, R. and Anderson, E. E., "Heat Transfer in Semitransparent Solids," *Advances in Heat Transfer,* Vol. 11, 1975, pp. 317-441.

[15] Jeans, J. H., "The Equations of Radiative Transfer of Energy," *Monthly Notices of the Royal Astronomical Society,* Vol. 78, 1917, pp. 28-36.

[16] Cheng, P., "Two Dimensional Radiating Gas Flow by a Moment Method," *AIAA Journal,* Vol. 2, Sept. 1964, pp. 1662-1664.

[17] Cheng, P., "Dynamics of a Radiating Gas with Application to Flow over a Wavy Wall," *AIAA Journal,* Vol. 4, Feb. 1966, pp. 238-245.

[18] Schmidt, E. and Gelbard, E. M., "A Double P_N Method of Spheres and Cylinders," *Transactions of the American Nuclear Society,* Vol. 9, 1966, pp. 432-433.

[19] Bayazitoglu, Y. and Higenyi, J. K., "Higher Order Differential Equations of Radiative Transfer: P_3 Approximation," *AIAA Journal,* Vol. 17, April 1979, pp. 424-431.

[20] Higenyi, J. K. and Bayazitoglu, Y., "Radiative Transfer of Energy in a Cylindrical Enclosure with Heat Generation," *AIAA Journal,* Vol. 18, June 1980, pp. 723-726.

[21] Ratzel, A. C., "P-N Differential Approximation for Solution of One- and Two-Dimensional Radiation and Conduction Energy Transfer in Gray Participating Media," Ph.D. Dissertation, University of Texas, Austin, 1981.

[22] Pomraning, G. C., "Radiative Transfer via Spherical Harmonics," *Transport Theory and Statistical Physics,* Vol. 8, 1979, pp. 67-97.

[23] Modest, M. F., "A Simple Differential Approximation for Radiative Transfer in Nongray Gases," *Journal of Heat Transfer,* Vol. 101, Nov. 1979, pp. 735-736.

[24] Kung, H. C. and Sibulkin, M., "Radiative Transfer in a Nongray Gas Between Parallel Walls," *Journal of Quantitative Spectroscopy Radiative Transfer,* Vol. 9, Oct. 1969, pp. 1447-1461.

[25] Yuen, W. W. and Rasky, D. J., "Application of the P-1 Approximation to Radiative Transfer in a Nongray Medium," *Journal of Heat Transfer,* Vol. 103, Feb. 1981, pp. 182-184.

[26] Marshak, R. E., "Note on the Spherical Harmonics Method as Applied to the Milhe Problem for a Sphere," *Physical Review,* Vol. 71, April 1947, pp. 433-446.

[27] Anderson, J. D., "Nongray Radiative Stagnation Point Heat Transfer;" *AIAA Journal,* Vol. 6, April 1968, pp. 758-760.

[28] Miele, A. and Iyer, R. R., "General Technique for Solving Non-Linear, Two Point Boundary-Value Problems via the Method of Particular Solutions," *Optimization Theory and Applications,* Vol. 5, May 1970, pp. 382-399.

[29] Yücel, A., "P-N Approximation for Radiative Transfer in a Nongray Planar Medium," Ph.D. Dissertation, Rice University, Houston, Texas, May 1982.